



## Research Paper

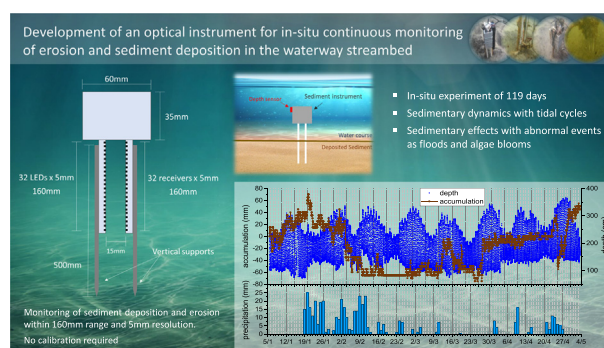
## Development of an automated sensor for in-situ continuous monitoring of streambed sediment height of a waterway

T. Matos<sup>a,\*</sup>, J.L. Rocha<sup>a</sup>, C.L. Faria<sup>a</sup>, M.S. Martins<sup>a</sup>, Renato Henriques<sup>b</sup>, L.M. Goncalves<sup>a</sup><sup>a</sup> MEMS-UMinho, University of Minho, Campus de Azurém, Guimarães, Portugal<sup>b</sup> Institute of Earth Sciences, University of Minho, Campus de Gualtar, Braga, Portugal

## HIGHLIGHTS

- An automated in-situ instrument for monitoring of streambed sediment height
- Optical sensor with 16 cm measuring range, 5 mm resolution and no calibration needed
- Autonomy above 1 year with continuous measurements at a 5/min sample rate
- Detection of sediment deposition and re-suspension patterns due to tidal cycles
- Abnormal erosion during floods and high sediment accumulation rates with algae blooms

## GRAPHICAL ABSTRACT



## ARTICLE INFO

## Article history:

Received 7 September 2021

Received in revised form 29 November 2021

Accepted 30 November 2021

Available online 4 December 2021

Editor: Fernando A.L. Pacheco

## Keywords:

Sediment deposition  
erosion  
Optical sensor  
Oceanography

## ABSTRACT

The sedimentary processes play a major role in every aquatic ecosystem, however, there are few automated options for in-situ monitoring of sediment displacement in the streambed of waterways. We present an automated optical instrument for in-situ continuous monitoring of sediment deposition and erosion of the streambed that requires no calibration. With a production cost of 32€, power consumption of 300  $\mu$ A in sleep mode, and capacity to monitor the bedform of a waterway, the sensor was developed to evaluate the sediment dynamics of coastal areas with a wide spatial and temporal resolution. The novel device is intended to be buried in the sand and uses 32 infrared channels to monitor the streambed sediment height. For testing purposes, a maximum measuring length of 160 mm and 5 mm resolution was chosen, but these values are scalable. Sensors can be built with different ranges and precision according to the needs of the fieldwork. A laboratory experiment was conducted to demonstrate the working principle of the instrument and its behaviour regarding the turbidity originated by suspended sediment and the settling and deposition of the suspended particles. The device was deployed for 119 days in an estuarine area and was able to detect patterns in the sediment deposition and resuspension during the tidal cycles. Also, abnormal events occurred during the experiment as floods and algae blooms. During these events, the sensor was able to record exceptional erosion and sediment deposition rates. The reported automated instrument can be broadly used in sedimentary studies or management and planning of fluvial and maritime infrastructures to provide real-time information about the changes in the bedform of the watersheds.

## 1. Introduction

Sediment deposition occurs when the water flow is slow enough so the particles (suspended load or bedload) can no longer be supported by the water turbulence, making it settle down at the bottom of the water body. The suspended particles that fall to the bottom of a water body are called

\* Corresponding author.

E-mail address: [matos.tiagoandre@cmems.uminho.pt](mailto:matos.tiagoandre@cmems.uminho.pt) (T. Matos).

settleable solids (Alber, 2000). As they are found in riverbeds and streambeds, these settled solids are also known as bedded and accumulated sediment. Sediment deposition can be found anywhere in a water system, from high mountain streams to rivers, lakes, deltas, floodplains and sea bottom. The size of settleable solids varies by the zone of the watershed. In high flow areas, larger and heavier gravel-sized sediment are expected to settle out first. Finer particles, including silt and clay, are carried all the way out to the estuarine areas where will settle or remain in circulation due to the action of the river and sea currents (Dyer, 1995).

In marine environments, nearly all suspended sediment will settle due to the presence of salt ions in the water. Salt ions bond to the suspended particles, attaching them to each other. As the weight of the flocculated particles increases with the increase of the salt, the sediment begins to sink to the seafloor. This is one of the reasons why oceans and other marine ecosystems tend to have lower turbidity levels (high water clarity) than freshwater environments. However, while estuaries and other tidal areas may be considered marine, the water in these locations is not necessarily clearer than freshwater. Estuaries are the collection point for suspended sediment coming down the rivers. Furthermore, in a tidal zone, the constant water movement causes the bottom sediment to continually resuspend, preventing high water clarity during tidal periods. Besides the density of suspended sediments, the clarity of an estuarine is also highly influenced by its salinity level, which leads to an increase in sediments deposition (Håkanson, 2006).

Many ecosystems benefit from sediment deposition. Sediment builds aquatic habitats for spawning and benthic organisms and is also responsible for providing nutrients to aquatic plants, as well vegetation in nearshore ecosystems (Galloway et al., 2005). While sediment is needed to build aquatic habitats and reintroduce nutrients for submerged vegetation, too much or too little sediment can easily cause an imbalance in the ecosystem and safety issues. Some aquatic habitats are even grain-size specific and require a specific sediment size, such as gravel, since too fine sediment can end up smothering the eggs and other benthic creatures (Chazottes et al., 2008; Auld and Schubel, 1978; Wenger et al., 2014; Rabeni and Smale, 1995).

Regular sediment deposition can be a support for aquatic habitats, but high sedimentary accumulation can also unbalance or destroy ecosystems. Siltation, the name for fine sediment deposition, occurs when water flow rates decrease dramatically. These deposited particles can also alter the waterway banks and channels direction when an unusually high sediment load settles out. Sediment deposition is responsible for creating alluvial fans and deltas, but excessive accumulation of sediment can build up channel plugs and levees. These deposits can block the river from reaching other stream threads or floodplains, which is not only an environmental issue but also a frequent problem for vessels, due to the formation of shallows in the navigation channels, as sediment siltation in harbours and marines that inevitably leads to dredging operations (Van der Wal et al., 2011).

Though too much sediment is the most common concern, the lack of sediments in the waterway may also lead to environmental issues. Sediment starvation is often caused by man-made structures, such as dams, or by natural barriers that limit sediment transport (Ćosić-Flajsig et al., 2020). Without sediment transport, and deposition, new habitats cannot be formed since it will lead to nutrient depletion in floodplains and marshes, and submerged vegetation cannot grow (Barko et al., 1991). Also, while water clarity is often pointed to as water quality, low amounts of turbidity cannot protect aquatic species from predation. Too little sediment can alter an ecosystem to the point that native species cannot survive (Wilson, 1990).

In addition to the effects on aquatic life, the loss of sediment transport and deposition can cause physical changes in the terrain. Downstream of dammed rivers, it is common to see receding riparian zones and wetlands due to the loss of transported sediment (Tuckerman and Zawiski, 2007; Yang et al., 2006). Erosion downstream of a barrier is common, as is coastline erosion when there is not enough sediment carried by the rivers. When this happens, the flowing water will pick up new sediment from the bottom and banks of the waterway (eroding instead of refreshing habitats), as it attempts to adjust to a uniform flow rate. Too little sediment deposition can lead to the erosion of riverbanks and coastal areas, causing land loss and

destroying the nearshore habitats. Without sediment deposition, sandy lowland coastal zones become eroded or migrate inland (Rachold et al., 2000; Hsu et al., 2007; Van Rijn, 2011).

The monitoring of sedimentary processes is essential, not only to support the project and management of maritime and fluvial infrastructures but also to protect the aquatic life and safeguard its water quality (Aminoroayaie Yamini et al., 2018). Continuous monitoring can be useful for the quantification of sediment in the seaside zone and for understanding the evolution of the littoral coast, therefore, it becomes essential for an effective study in each area of action.

Even though the deposited sediment monitoring is an important variable in sedimentary studies, the current state of the art still relies on collecting field samples with mechanical systems as bottles, traps, pump samplers or sample dredgers for posterior laboratory analysis (Håkanson et al., 1989; Storlazzi et al., 2011). One of the problems of these mechanical traps and collectors of sediments is that their structural housing causes hydrodynamic disturbance in the normal flow of the waterway which results in a lower chance of the normal sediment resuspension. Therefore, it provides a gross estimate of sedimentary rates. The other, and the major concern about these techniques, is that discrete sediment sampling does not allow sedimentary processes to be observed with continuity, thus limiting their understanding. This problem opened space for new and automated instruments that aim to perform continuous monitoring of bedform evolution in-situ.

In the last decades, the scientific community has been trying to overcome the lack of automated instruments to measure the accumulation of streambed sediments. The measurement of deposited sediment by electric conductivity was firstly reported (Ridd, 1992). Later, a device was developed using a settling plate with two electrodes that change the electric conduction depending on the thickness of the accumulated sediment (De Rooij et al., 1999). In 2009, a vertical array of electrodes was proposed using the electrical response of the sediment-water interface to find the sediment-water boundary (Arnaud et al., 2009). Although these techniques are accurate, all of them require precise calibration and the sensor outputs are highly dependent on variables as water depth, conductivity of the medium and sediment characteristics. Slight fluctuations of any of these parameters can significantly affect the accuracy of the readings.

An optical sensor to measure the thickness of sediment accumulation was presented using the backscattering technique to measure the amount of sediment that settles in a deposition plate (Thomas and Ridd, 2005; Ridd et al., 2001). The backscattered light power is used to estimate the amount of sediment accumulated over that given area. One of the limitations of the apparatus is the smoothness of the deposition plate that results in rapid resuspension and makes it impossible to take accurate measurements with high flows. An improvement of the instrument was presented in 2017, with a surface more closely approximated to the complex and typically rugose microtopography of a coral surface (Whinney et al., 2017). The principal problem with these instruments is that can only measure the settled sediment at a given time and do not provide any information about resuspension rates or erosion.

The Photo-Electronic Erosion Pin (PEEP) system was presented (Lawler, 1991). Later, the Surface Elevation Dynamics (SED) sensor was also proposed (Hu et al., 2015). Both these two instruments use a vertical array of optical receivers to detect the boundary where the receivers can no longer detect natural light (these detectors would be buried with sediment). However, these instruments are dependent on the natural light and cannot take measurements during the night, at high depths, or in water with high turbidity where the natural light cannot reach.

Finally, acoustic technologies have also been used to monitor bed elevation using the underwater acoustic altimetry principles (Gallagher et al., 1996; Jestin et al., 1998). For these methods, high frequencies must be used to achieve high sediment accumulation resolutions, which increases the vulnerability to undesired echoes by the suspended sediment in the water and limits its applications.

We have been presenting innovative monitoring instruments to measure sedimentary processes in the marine environment (Matos et al.,

2019a, 2020). These technologies have been developed with three major manufacturing concerns. First, to be low cost and allow massive replication and deployments with a high spatial resolution. Second, to be low power and enable a long time continuous monitoring without replacement of batteries. And third, to make the instruments small and light for ease of installation and reduced maintenance. A multipoint optical instrument to measure turbidity and sediment transport was presented before. Although the device was inspired by the technology of another optical sensor to measure turbidity, suspended particulate matter and distinguish between organic and inorganic suspended sediment, the results of both laboratory and field experiments showed potential to measure the process of sediment accumulation in-situ.

Inspired by the results of the previous multipoint optical instrument, we now present a new and innovative automated apparatus, totally focused on the continuous in-situ monitoring of sediment deposition and erosion in the streambed of a waterway. This new instrument aims to fill the need for automated instruments to monitor these two sedimentary processes in the bed of the waterways and must be able to perform continuous monitoring for some months. We believe that this new device can be broadly used, not only in field studies, like the one we presented, but can also provide a significant impact on the monitoring and managing of fluvial and marine infrastructures affected by silting, like dams, harbours or navigation channels, or by scour and other erosion problems like bridges or offshore structures.

The manuscript is divided into the **Materials and Methods**, **Results**, **Discussion** and **Conclusion** sections. **Materials and Methods** explain the principle of work of the sensor, the electronic and mechanical design to allow its replication to the Scientific Community, and the methodology

for the in-situ experiment. The **Results** section analyse the measurements recorded by the sensor during the in-situ deployment and take into consideration the sedimentary processes detected. The **Discussion** section highlights the major achievements of the development instruments and makes recommendations for future deployments and changes in its design. A summary of the developed work and final considerations are made in the **Conclusion** section.

## 2. Materials and methods

### 2.1. Sensor development

With the main objective to provide reliable and accurate data about sediment accumulation in marine and fluvial environments, we propose an innovative low-cost and low-power apparatus. The instrument is intended to be buried in the streambed of the waterway and offers a maximum measuring length of 160 mm and 5 mm resolution to continuously monitor sediment deposition and erosion. The developed sensor uses 32 infrared (IR) transmitted light emitter-receiver pairs with 5 mm displacement, which results in a sensing length of 16 cm. As Fig. 1 shows, the optical transducers are separated into two printed circuit boards arrays (one for the IR emitters and the other for the IR receivers) that are placed in front of each other, displaced by 15 mm, and with the emitter-receiver pairs aligned (principle of transmitted light detection).

The instrument is intended to be buried in the streambed and this is the configuration that allows measuring the height of deposited sediment or height decrease by sediment resuspension or erosion. One at a time, each one of the 32 nodes emits light from the emitter to the receiver. If the

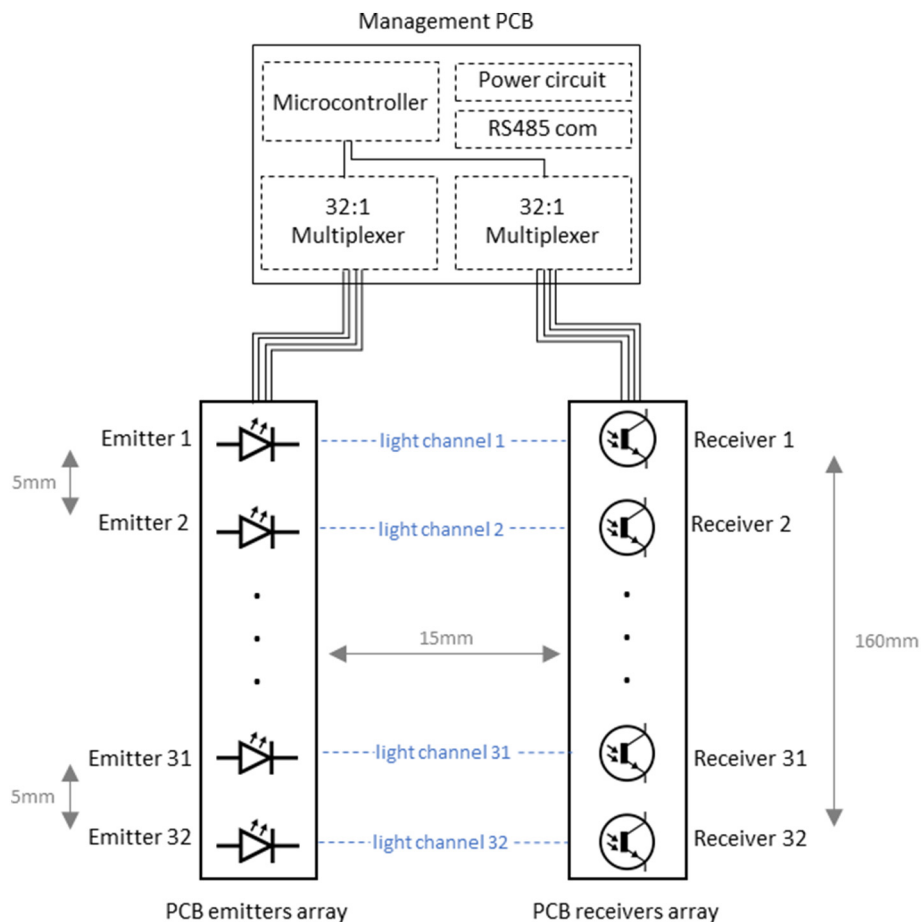


Fig. 1. Schematic of the 32 light channels of the sensor. It uses two aligned printed circuit boards (PCB), displaced by 15 mm, with arrays of 32 light emitters and 32 light receivers, respectively. Each one of the nodes is displaced 5 mm from the adjacent, resulting in a maximum sediment accumulation measuring length of 160 mm. A third printed circuit board is used with the power, instrumentation and processing circuits.



receiver senses the light emitted by its pair, it means that the channel is clear. When the emitting light cannot reach the light detector, it means that the channel is obstructed by sediments. Analysing the electrical output of each receiver, the sediment height is computed based on the number of detectors that can no longer detect light. It is important to notice that the sensibility of the emitter-receiver pairs is designed so that in water with 4000NTU the light sensed by the receivers is higher than zero. This means that the sensor can properly work in water with high turbidity.

For the hardware, and to achieve the 5 mm resolution, small packages are used for the light emitters and receivers. The light-emitting diode (LED) APT2012F3C (940 nm, 120° emitting angle and 1.2 mW/sr radiant intensity at 20 mA) is used for the light-emitting sources and the phototransistor APT2012P3BT (940 nm, 160° view angle and 100 nA dark current) for the light receivers. The good performance of infrared LEDs and phototransistors in this type of sensing instrument to monitor sediment processes was already documented in previous work (T. Matos et al., 2019b, 2020). To select the 32 light channels, the low-power microprocessor stm32L496ZG and two 1:32 bidirectional multiplexer ADG732BSUZ (one for each PCB array) are used to control the LEDs switch and read the analogue output of the phototransistors. Finally, a low power rs485 driver LTC1480 is used for the digital output of the sensor and is intended to be connected to a data logger. The electronics schematics can be consulted in Fig. S1, Supplementary Materials.

The sensor is intended to be supplied by a common 3.6 V Li-Ion battery, so for the power supply circuit, the low-dropout regulator LDK320AM30R (3 V fixed output, 200 mA max current, 100 mV dropout voltage and 60  $\mu$ A quiescent current) is used. The developed hardware has a power consumption of approximately 25 mA during the readings (the sensor takes 35 ms to read the 32 channels and process the accumulation value) and 300  $\mu$ A in sleep mode. This means that using a common mobile phone 3000 mA  $\times$  3.6 V lithium battery, the sensor has an autonomy of more than 1 year to take continuous measurements at a 5/min sample rate.

To comprise the electronic printed circuit boards and to meet the water-tight needs for full submersion, the structural housing of the sensor is filled

with epoxy (HB Quimica - EPOSURF 2). Two vertical steel supports of 50 cm are fixed on the side of each array for higher robustness of the sensor to the water flow strength during the in-situ measurements. One of the main objectives during the manufacturing of the device was to be low-cost to allow massive replication. The presented instrument has a manufacturing cost of 32€ in raw materials used for the electronic components and structural housing. The mechanical drawing of the sensor can be consulted in Fig. S2, Supplementary Materials.

## 2.2. Laboratory experience

A laboratory experiment was conducted to evaluate the operation of the developed instrument. To simulate the sediment deposition process that occurs in situ, the instrument was buried in a cylindrical recipient with seashore sand and water. As Fig. 2 shows, seashore sand was slowly added to the recipient to simulate the sediment deposition and consequently cover all the optical channels of the instrument. Fig. 3 presents the output voltage obtained in the top and bottom sediment sensor of the device, during this test.

As explained in Sensor Development Section, the optical channels are built in a transmitted light detection configuration (LED aligned with the receptor). The typical response of this type of measurement is a high electrical output for low turbidity measurements and a low electrical output for high turbidity values. The turbidity is influenced by the suspended sediments in the sample that blocks the passage of the light emitted by the LED and result in less light detected by the receiver. A full study about the response of this light-sensing technique, as for nephelometric and back-scattering techniques, was presented before (Matos et al., 2019b).

During the experiment, the instrument was taking records of each optical channel at a sampling frequency of 2 Hz. One at a time, each one of the 32 LEDs was turned ON, and the electrical output of the corresponding optical receiver was recorded. Fig. 3 shows the measurements taken for the top (further away from the sand) and bottom (closer to the sand) channels

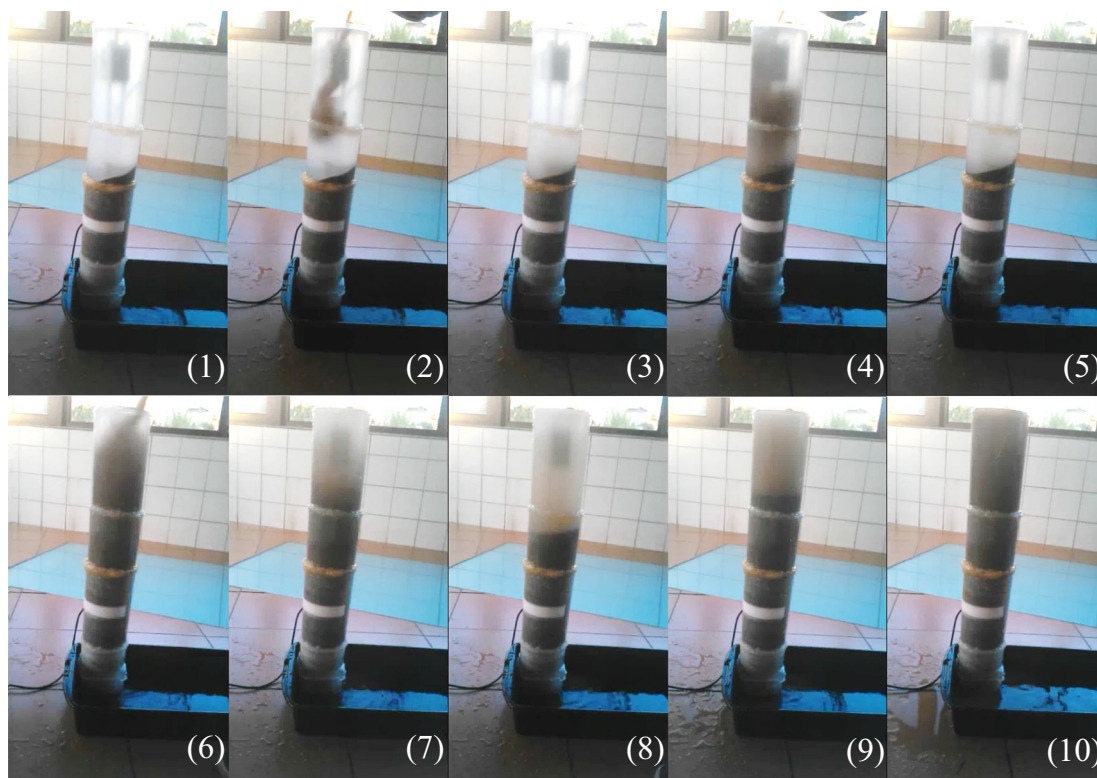


Fig. 2. Laboratory test of the sediment accumulation sensor. The instrument was buried vertically in a recipient with seashore sand and water (1). Seashore sand was slowly added to the recipient to increase the sediment deposition (2–9) until the instrument became covered (10).

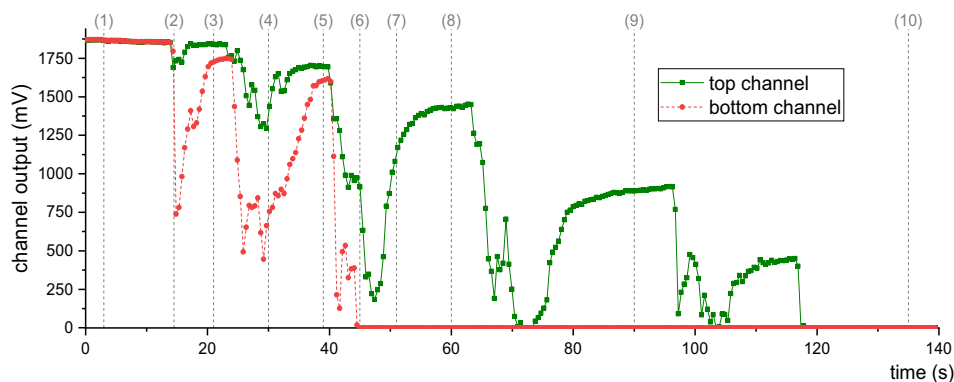


Fig. 3. Laboratory test of the sediment accumulation sensor. The measurements of the top channel (green square and solid line) and bottom channel (red circle and dash line) were recorded while the device has been buried with seashore sand. The time marks in the top horizontal axis correspond to the image labels of Fig. 2.

of the device. The time marks in the top horizontal axis correspond to the image labels of Fig. 2.

The typical behaviour of the transmitted light technique was reflected during the experiment. In the graph of Fig. 3, higher output voltages correspond to lower turbidity values. The test started with the sensor vertically placed in the recipient with seashore sand and water, and with all the optical channels uncovered (time (1)). This time corresponded to the less turbidity point during the experiment, and so the high electrical output was recorded by both channels. In the first drop of sand (time (2)), both channels detected an abrupt decrease in the electrical output caused by the settling of the heavier particles. Then, while the remaining sediment settles in the bottom, the turbidity decreases (time (3)). This behaviour was repeated during all the experiments (sand drops at (4) and (6) and settling periods at (5) and (7–9)). The bottom channel became buried at (6) and the top channel sensor at (10).

It is important to notice that the output decrease rate is higher for the bottom channel than for the top channel because while the sediment is settling, the turbidity decreases from the top of the container to its bottom (as is perceptible in Fig. 2). Also, the turbidity of the water in the container gets higher at each drop of sand (see the difference between (1), (3), (5), (8) and (9)). This happens because while the heaviest particles settle in the bottom, the finer and light sediment particles do not have time to settle and contributes to the increase of turbidity (in Fig. 2 it is possible to visually interpret the differences in the water clarity at the different times).

Even with high turbidity levels, the channels were still able to detect changes in turbidity, at least until the channel output was zero. When this happened, the emitting light could no longer reach the optical receiver, which means that the channel was buried in the sand. The bottom channel was the first to become buried (Fig. 3 at 45 s) and the top channel the last one (Fig. 3 at 119 s). The other 30 optical channels became buried in between this range of time, and this is the principle that makes the developed instrument suited to measure sediment accumulation in the streambed of a waterway and do not need any kind of calibration to be operated (the reference that corresponds to deposited sediment in the channels is always zero). While in most of the electronic sensors there is a need to correspond the electrical output to a physical variable, for this sensor the electrical output of each channel indicates if it is blocked or not (covered with sediment or not). This means that each one of the optical channels has a binary output. The sediment height is then computed based on the number of following channels that cannot detect the correspondent emitted light (starting from the bottom to the top).

Fig. 4 shows the records of all 32 channels, as well the level of sediment accumulation that represents the final output of the device. Note that in an ideal instrument, with standardized product quality, the output of all the 32 channels should be the same for the same water sample (in this case, in time 0, before the seashore sand is dropped). Turbidity discrepancies are found

between the readings between the 32 channels. These are due to electronic component tolerances, and differences in the alignment of the optical transducers. Nevertheless, the sensor output (sediment accumulation, in the bottom graph of Fig. 4) is not affected since the sensor was designed to be immune to these variations. Electronic components with high tolerances can be used, and precise alignment of optical components is not necessary, thus achieving lower costs for the same performance.

As demonstrated in Fig. 4, while all the channels are uncovered, the output of the instrument is 0 mm. However, when the bottom channels become buried, the accumulation output increases to a maximum of 160 mm (32 channels with 5 mm resolution). The output of each channel is used to compute the sediment height, allowing to detect sediment deposition and erosion.

This experiment was conducted to test the developed instrument in a simulation of a fast sediment deposition that would increase the sediment accumulation in the streambed. All the behaviour demonstrated in this experiment, both for turbidity and sediment deposition, are phenomena that are expected to occur during in situ deployments, at a lower deposition rate.

### 2.3. In-situ deployment

The device was installed, from 5 January to 3 May 2021, in the estuary of Cávado river, Esposende - Portugal (41°31'56.6" N 8°47'04.8" W). This location was chosen due to its high sedimentary dynamic, where the formation of shallows is constant, and the geomorphology of the area is continually changing. The same spot was used in the past to evaluate the performance of the previously developed instruments to measure sediment processes (Matos et al., 2019b, 2020).

The instrument was connected to a data logger that received and stored the monitoring information with a sampling rate of 30 min, using the RS485 communications protocol. The developed device was vertically buried in the estuary streambed, with channels 1 to 19 uncovered, and the remaining 13 nodes buried in the sand (see Fig. S3, Supplementary Materials). Channel 20 was defined to correspond to 0 mm of sediment accumulation. With this configuration, the instrument would be able to measure not only the periods when the suspended sediments are settling (accumulation will increase and the optical channels will be covered with sand) but also when the deposited sediments resuspend due to the action of sea currents or the river flow (the streambed will erode and the optical channels will be uncovered).

During the experiment, the sensor had exceeded its measuring range two times. For the first time, a flood caused an abnormal erosion in the streambed of the estuary and all the 32 optical nodes became uncovered. In the second one, the opposite occurred and all the 32 nodes became buried in sediment. For both cases, the sensor had to be repositioned with half of the optical array covered and the other half uncovered, so it could measure sediment deposition and erosion again. Repositioning means that the

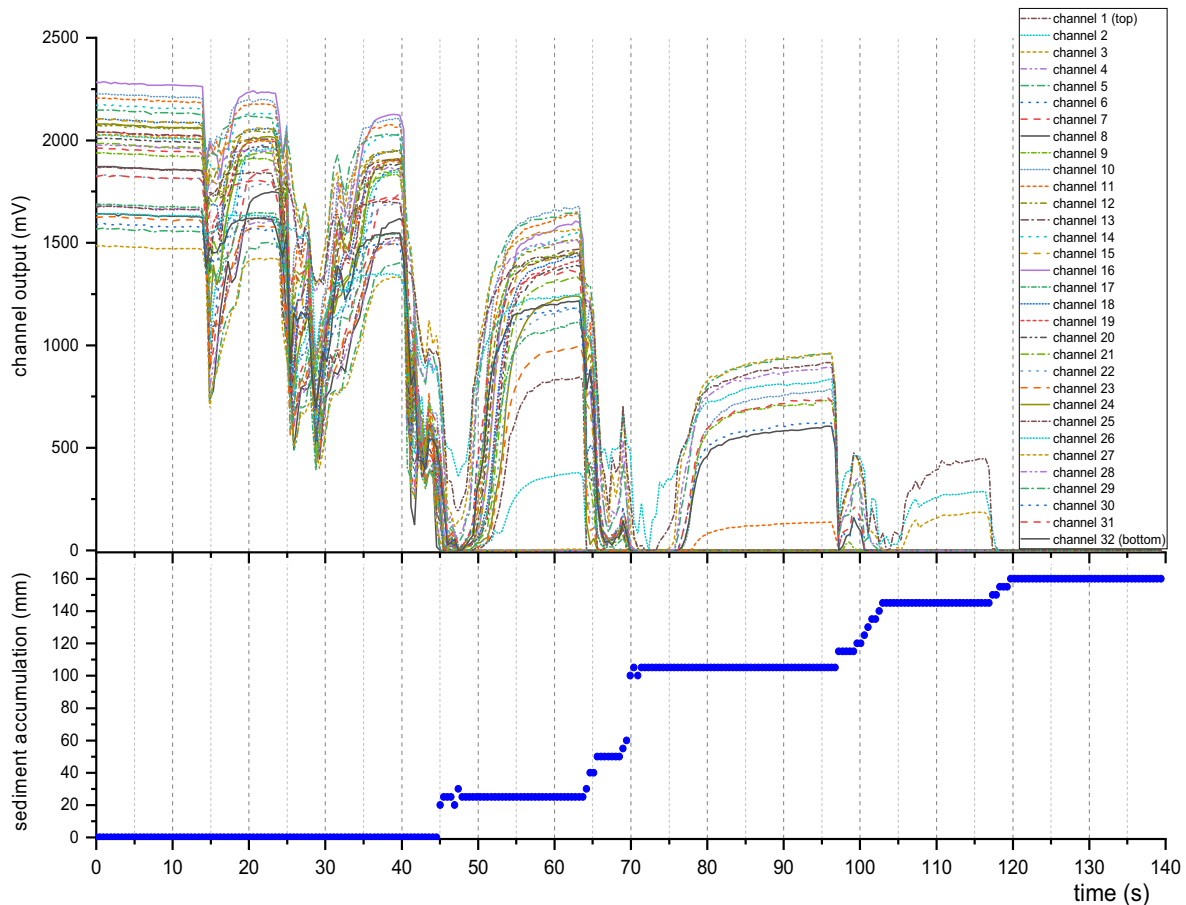


Fig. 4. Electrical output recording of each of the 32 optical channels during the laboratory experiment in the top graph and processing of the sediment accumulation in the bottom graph.

sensor was moved only vertically. During the field experiment, the sensor was always in the same spot in the estuary. For the first case when the nodes were all uncovered, the sensor was pushed to the sand so it became half buried again. For the second case when the nodes were all buried, the sensor was lifted from the sand. Every time the sensor was repositioned, the optical nodes in the sand-water frontier were defined as the previous sediment height measured so that the measurements had a continuation.

Complementarily, a water level sensor was used to obtain the height of the water column by measuring the pressure from bottom to top and detecting water level fluctuations due to tide cycles. These data were used to correlate the accumulation measurements with the hydraulic dynamics of the zone. The water depth sensor was attached to the top of the sediment accumulation sensor, in a fixed position, with the zero-depth arbitrary defined as the position of the sensor at the moment of the installation. This setup was used only for field test purposes, without aiming to obtain datum-based values of water or sedimentation depths. In further monitoring studies with the developed instrument, the top position of the sediment sensor should be collected with the Global Navigation Satellite System (GNSS) and calibrated considering the measurement of data from the national geodetic network. As we present in the next section, the weather also had significant relevance in the sedimentary processes detected, so the daily precipitation rate is presented. The precipitation data was taken from Instituto Português do Mar e da Atmosfera (IPMA).

### 3. Results

Fig. 5 shows the measurements of the developed sensor and the water depth during the first week of deployment. The sediment accumulation,

starting at 0 mm that corresponds to the optical channel 20 as defined before, is represented in the left-side y-axis with brown circles and a brown solid line. In the right-side axis and with blue circles is presented the data from the depth sensor and consequently the tidal cycles in the estuary of Cávado river. Analysing the first days of the in-situ test, even that does not happen during all the tidal cycles, seems to have a pattern that is reflected in a high sediment deposition during the high tide (accumulation increases) and sediment resuspension during the low tide (accumulation decreases).

This behaviour match with one of the phenomena expected in this estuarine area. During the low tide, the sea currents have minimal or no effect at all in the normal flow of the river. However, when the tide increases the normal river flow strength is diminished by the sea entering throughout the estuary and it can be not only cancelled but also overcome. During the peak of the high tide, lower water flow strength is expected and the water in the estuary is saltier. Both these two conditions contributed to the settling of fine particles that were suspended in the water, which led to an increment of the accumulated sediment in the streambed. Once the tide started to decrease, the river flow increased and its maximum strength happened during the low tide. At this time, the flow strength is higher than during the high tide, so the fine sediment that has settled before enters now in resuspension in the direction of the sea. This behaviour was recorded in the monitoring data of the sensors during all 119 days of deployment.

During the first fortnight of the field tests, the sensor was recording an increase of the accumulated sediment in the streambed of the estuary, reaching a maximum of 70 mm on 20th January. However, this date also marked the start of 4 weeks of intense precipitation, when the sediment accumulation sensor detected an abrupt decrease in its measurements (see Fig. 6).

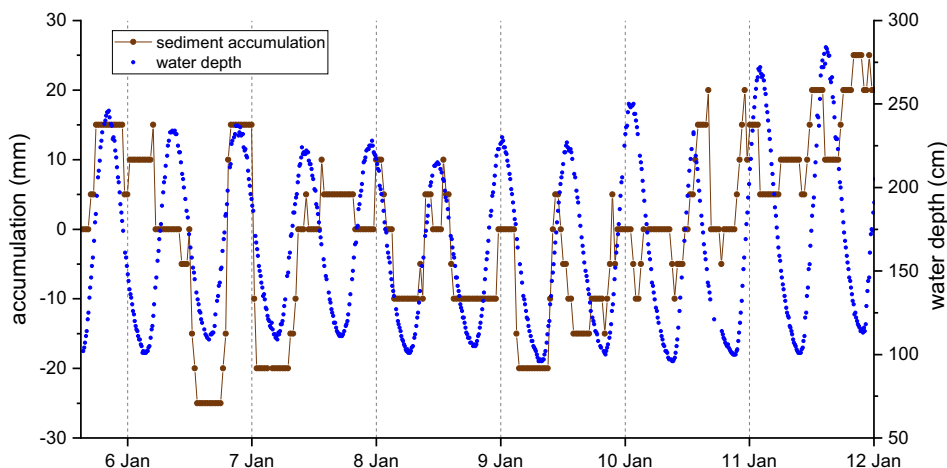


Fig. 5. Monitoring results of sediment accumulation and water depth in the first week of deployment (5th of January to 12th of January 2020). The brown circles with the brown solid line are the data output of the sediment accumulation sensor (left side y-axis). The blue circles represent the data from the depth sensor and show the tidal cycles in the estuary (right side y-axis).

On rainy days, the volume of water in the river increase. As Fig. 6 shows, the depth sensor recorded the river flow increasing from 20th to 30th of January, 3rd to 5th of February and from 9th to 12th February (notice that in these days, the depth during the peak of the low tide was higher than the expected, which means that the estuary had an abnormal higher water volume). Particularly in rivers that pass by urban areas, as is the case of the Cávado river, not only additional water is added to the waterway, but also mud and waste that runoff from the riverbanks and that is drained from its surroundings. In these conditions, the river gains high kinetic energy that results in a higher water velocity and turbulent flow.

These abnormal conditions in the estuary do not follow the normal balance of sediment deposition and resuspension shown in Fig. 5. The high strength of the river course resulted in the erosion of the streambed at an unusual rate. From the 20th of February, when the sensor registered a maximum of 70 mm of accumulated sediment, to the 10th of February, when

the sensor was measuring  $-65$  mm, the streambed of the estuary eroded an unexpected 135 mm and all the 32 channels of the sediments instrument became uncovered.

From 10th to 18th February some sediment deposition was recorded, also the resuspension of that sediment. However, the device was on its measurement length limit (the starting position in the deployment of 13 channels uncovered, with a resolution of 5 mm, results in an erosion measurement limit of  $-65$  mm) and no other changes were recorded till the 26th of February.

Fig. 7 shows underwater photographs of the sensor at the beginning of the installation and on the 26th of February when the sensor could not take more reliable measurements since all channels were uncovered. Analysing the images, it is possible to notice differences in the type of sediment deposited in the estuary bed. In the left image (beginning of the installation) the streambed sand had linguoid ripple marks and its surface was uneven. However, this layer of thin sand disappeared on the middle and right

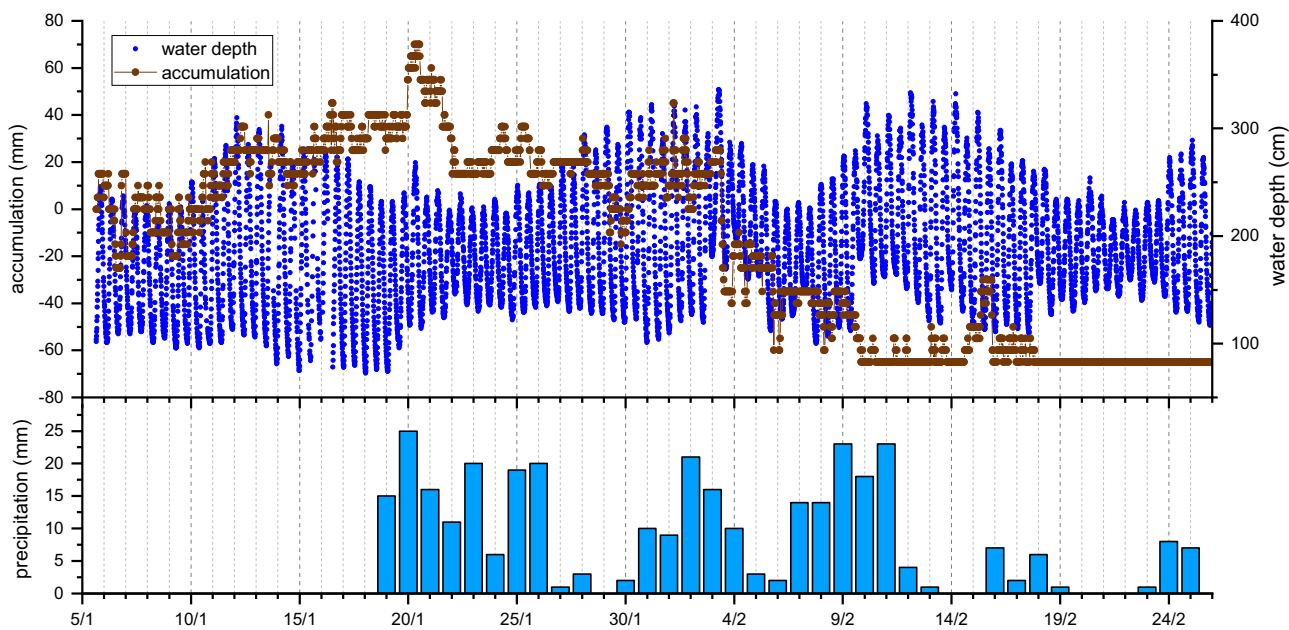


Fig. 6. Monitoring results of sediment accumulation and water depth from 5th of January to 26th of February 2020. In the top graph, the data from the sediment accumulation in brown circles and brown solid line (left-side y-axis) and the data from the water depth sensor in blue circles (right-side y-axis). In the bottom graph, a bar chart with the daily accumulated precipitation.





**Fig. 7.** Underwater photographs of the sediment accumulation sensor at different times of the field test. In the image at left, the moment when the sensor was deployed, with its measure correspondent to 0 mm. In the middle image, the sensor could not provide reliable data anymore since all the 32 optical channels were completely uncovered (26th of February, measure correspondent to -65 mm). In the image at right, also on the 26th of February, the sensor was buried again in the same location (only the vertical position changed), and its measure continued with the value before of -65 mm.

images, and the streambed looks more swept due to the erosion caused by the days of strong precipitation.

On the 26th of February, the sensor was buried again in the sand, in the same location as before (it just changed the vertical position), with nodes 1 to 14 uncovered, as shown in the image at the right photograph of Fig. 7. To continue the previous measurement the sensor output was “zeroed”, with the optical channel 15 corresponding -65 mm. Fig. 8 shows the continuation of the measurements after the sensor was buried.

After the rainy days, the accumulation of sediment in the streambed slowly returned to the initial values. The accumulation rates during the low and high tides, as shown in Fig. 5, were recorded again, and a new pattern was possible observed related to the tidal cycles. Analysing the monitoring records of Fig. 8, it is possible to see that during the spring tide there was a tendency for higher deposition rates in the estuary. On the contrary, during the neap tide higher sediment resuspension and erosion was recorded.

The bulge of the ocean and its effects on the estuary during high tidal periods were observed in the data of the water level sensor, mostly in the average depth of the high tides. In the periods of the neap tides, the water level registered depth values between 200 and 250 cm during the peak of the high tide, while for the spring tides, some of the high tide peaks almost

reached 400 cm. This means that during the spring tides, the salinity level in the estuary is expected to be higher than during the neap tides, which is the possible cause for the high sediment deposition rates recorded during that period.

After the 28th of March, the sensor was on its top measuring limit (all the nodes became buried). The reason for this registered high-rate deposition is unknown, however, this period was marked by an increase of algae and high turbidity in the estuary that was not observed before, and that possibly is related to the occurred phenomena. The sensor registered sediment accumulation values in its top measuring limit until the 19th of April. At this date, the sensor was found in the estuary streambed, totally buried with sand and algae (see Fig. S4, Supplementary Materials). As before, the position of the sensor was adjusted so that sediment deposition and erosion was possible to monitor again. The sensor was buried with nodes 17 to 32 covered and 1 to 16 uncovered and its position was zeroed again.

Comparing the underwater photographs of Figs. 7 and S4, Supplementary Materials it is possible to notice the increase of turbidity, as also the green pigment in the water resulting from the presence of algae in the estuary (all photographs were taken with the same camera configurations, during the low tide and at similar weather conditions). In the photograph of Fig. S4, Supplementary Materials it is also possible to see that the structural

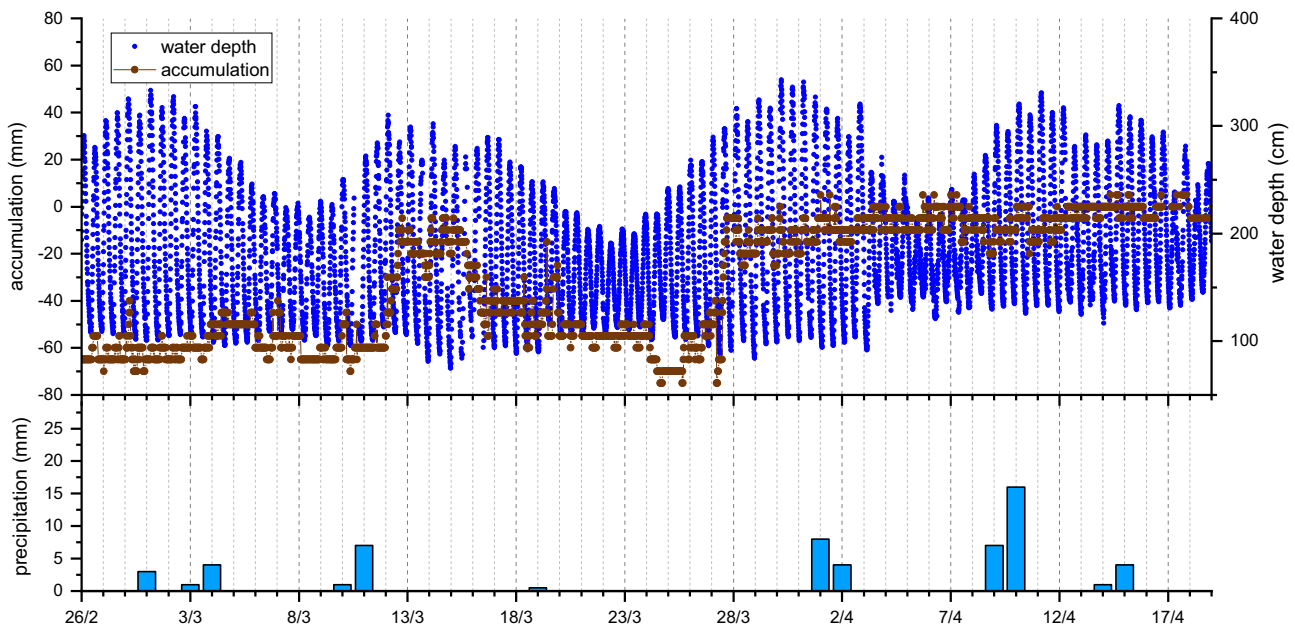


**Fig. 8.** Monitoring results of sediment accumulation and water depth from 26th of February to 19th of April 2021. In the top graph, the data from the sediment accumulation in brown circles and brown solid line (principal y-axis) and the data from the water depth sensor in blue circles (secondary y-axis). In the bottom graph, a bar chart with the daily accumulated precipitation.



housing that comprises the electronics were attached with macro fouling, but not the monitoring nodes (the sensor was not removed from the streambed and no cleaning was made).

After the repositioning of the sensor, the field experiment was conducted for 10 days, ending on the 3rd of May, when the sensor was again close to its measuring limit. Once again, this period was marked with high turbidity in the estuary and the existence of algae bloom, and the sensor registered an increase of sediment accumulation in the streambed. This high sediment deposition rate was only disrupted by the precipitation from the 21st to the 26th of April when bed erosion was registered. However, immediately after the precipitation days, the high deposition rates were recorded again.

Fig. 9 shows all the monitoring records of the sediment accumulation and water level sensors during the full field experiment in the estuary of Cávado.

#### 4. Discussion

During the in-situ experiment, the developed sensor showed its potential to monitor sediment deposition and erosion in the streambed of the river mouth. The new instrument was able to detect the sediment deposition and resuspension patterns originated by the ocean tides, both in high frequency (high tide – low tide) and in low frequency (spring tides – neap tides). Also, abnormal events as floods and algae blooms played a major role in the sedimentary processes during the experiment with high rates of streambed erosion and high sediment deposition rates, respectively.

The main objective of this work was achieved, developing a fully automated instrument capable of continuously monitoring the sediment height in the streambed of a waterway. While it does not provide qualitative information about the characteristics of the sediment as the mechanical samplers do, it can provide real-time information about the bedform changes (that as we could see during the experiment, it can change fast and cannot be detected by these methodologies of point collectors).

When compared to other automated technologies from the state of the art, the developed instrument was able not only to measure sediment deposition but also streambed erosion. This is an important advance since previous sensors based on deposition plates are not able to measure events of sediment resuspension (Thomas and Ridd, 2005; Ridd et al., 2001). The

presented sensor also offers minimal disturbance in the streamflow, is independent of external ambient light and can properly work in high turbidity waters, which is not the case of the PEEP and SED sensors (Lawler, 1991; Hu et al., 2015). Not requiring calibration is also a great advantage compared to the typical oceanographic sensors, which normally require complex and time consuming laboratory calibrations. The developed instrument is ready to be installed without any prior laboratory analysis.

During the presented field test, no maintenance was necessary for the good operation of the sensor, except on the 26th of February and 19th of April, when the sensor had to be repositioned again. The instrument was designed for a maximum measuring length of 160 mm, however, during these exceptional events, this range was not sufficient and the sensor had to be repositioned. However, its electronic design is highly scalable so setups with different combinations of lengths or resolutions can be built. Considering this, further optimizations should rethink the use of more optical channels to increase the range of the sensor.

We recommend maintaining the 5 mm of resolution since it provided reliable results. Another recommendation is to assemble the sensor in a fixed structure whenever possible (easiest to do when monitoring in infrastructures as harbours, dams or other platforms), to be sure that the sensor is not lifted due to high stream flows.

In the presented field experiment, the sensor was taking measurements at each 30 min. Even though results are satisfactory, in some periods, consecutive measurements presented a difference of 10 mm (higher than the 5 mm resolution), so we recommend increasing the sampling frequency in future in-situ deployments so that these transitions can be better detected.

Finally, during the deployment biofouling interference was not detected. It is known that optical devices are susceptible to biofouling and present errors during long time deployments without maintenance. Its effects have been analysed in the previous developed optical sensors for turbidity and suspended particle matter (Matos et al., 2019b, 2020). However, the new sensor that we present sets the threshold that defines if the optical channel is covered or uncovered in zero. This means that, even if both the optical emitter and the receiver presented biofilm on its surface, the instrument will still be able to calculate the sediment accumulation with reliability if the receiver can detect a minimal luminous power. During the

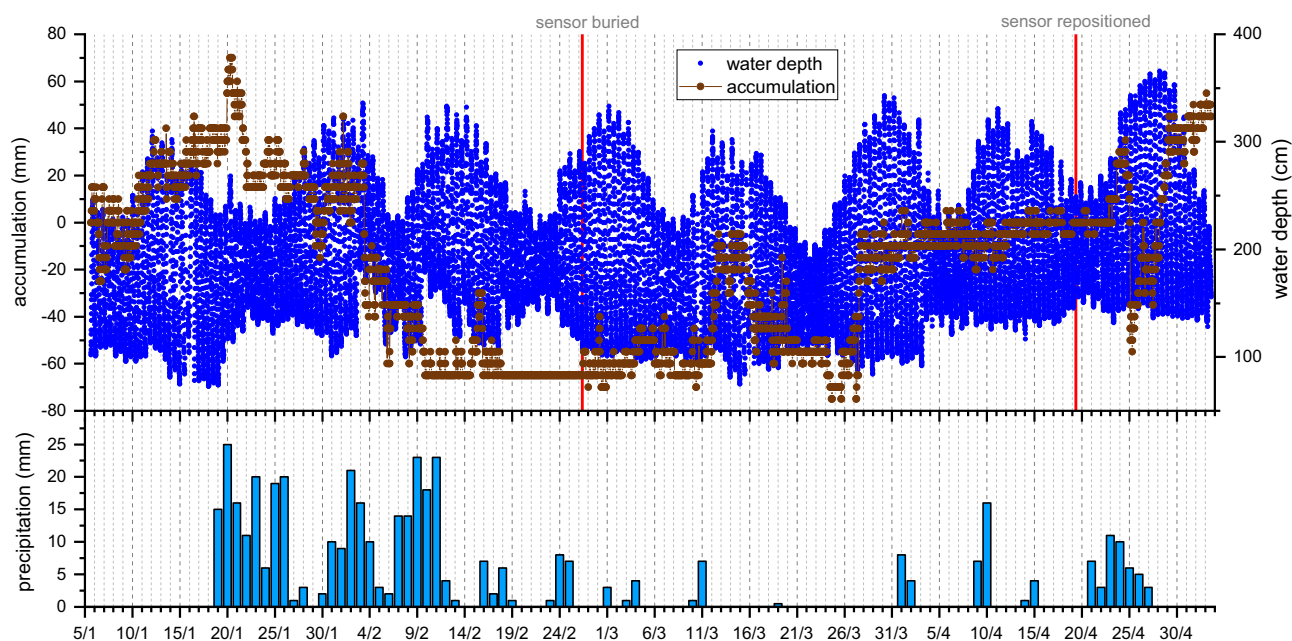


Fig. 9. Monitoring results of sediment accumulation and water depth from 5th of January to 3rd of May 2021. In the top graph, the data from the sediment accumulation in brown circles and brown solid line (principal y-axis) and the data from the water depth sensor in blue circles (secondary y-axis). The red line marks the moment when the device was buried again. In the bottom graph, a bar chart with the daily accumulated precipitation.

119 days of the field experiment, no biofouling interference was registered. Biofouling will only affect the light transmission channels when it blocks completely the light path between the emitter and detector, which is unprovable to occur. Moreover, if biofouling blocks any of the optical pairs above the sediment surface, malfunction can be detected since all channels above sediment surface must detect light and all channels below sediment surface must be blocked.

## 5. Conclusion

A low-cost, low-power and automated optical instrument is reported for in-situ continuous monitoring of sediment height of the waterway streambed. The device uses 32 infrared optical channels that are placed in a vertical array and allow the sensor to measure sediment deposition and erosion with a maximum measurement length of 160 mm and 5 mm resolution and does not require any calibration for in-situ deployments. The electronics, mechanics and methodologies for the proper work of the instrument are provided so it can be replicated by the Scientific Community.

The instrument was validated in deployment during 119 days in the estuary of Cávado river, an area with high sediment dynamics. The in-situ results showed that the sensor was able to detect patterns of sediment deposition and resuspension in the bed of the estuary during the low and high tides. The conducted deployment also experienced 3 weeks of intense precipitation that resulted in an abnormal increase of the river flow strength and floods. Due to these extreme conditions, the accumulation sensor was able to detect abrupt erosion in the estuary streambed that caused a decrease of 135 mm in the accumulated sediment in 20 days. Oppositely, in the last month of the experiment, the existence of algae bloom was observed in the estuary that led to high sedimentary rates. Due to inherent discrete measuring, it's expected that this instrument can be active for even longer periods, without being affected by biofouling.

The reported automated instrument can be used to deliver real-time data of the bedform changes and can provide significant impact in broad applications as sedimentary studies or managing and planning of fluvial and marine infrastructures affected by silting, like dams, harbours or navigation channels, or by scour and other erosion problems like bridges or offshore structures.

## CRedit authorship contribution statement

M.T.: conceptualization, methodology, software, hardware, validation, investigation, data analysis and writing original draft preparation; J.L.R.: depth sensor for the in-situ monitoring, field test support; F.C.L.: sensor structural housing and 3D printing; M.M.S.: review, editing and supervision; R.H.: validation, review and supervision; G.L.M.: review, editing and supervision. All authors have read and agreed to the published version of the manuscript.

## Funding

This work is co-funded by the project K2D - Knowledge and Data from the Deep to Space with reference POCI-01-0247-FEDER-045941, co-financed by European Regional Development Fund (ERDF), through the Operational Program for Competitiveness and Internationalization (COMPETE2020) and by the Portuguese Foundation for Science and Technology -FCT under MIT-Portugal Program. This work is also co-financed by Programa Operacional Regional do Norte (NORTE2020), through Fundo Europeu de Desenvolvimento Regional (FEDER), Project NORTE-01-0145-FEDER-000032 – NextSea, and by national funds through FCT – Fundação para a Ciência e Tecnologia, I.P. under project SONDA (PTDC/EME-SIS/1960/2020).

## Declaration of competing interest

The authors declare that they have no known competing financial interests or personal relationships that could have appeared to influence the work reported in this paper.

## Acknowledgements

The authors thank Câmara Municipal de Esposende and Museu Marítimo de Esposende for all the support and conditions provided for the realization of the field tests. T. Matos thanks FCT for grant SFRH/BD/145070/2019. C.L. Faria thanks FCT for grant SFRH/BD/137121/2018.

## Appendix A. Supplementary data

Supplementary data to this article can be found online at <https://doi.org/10.1016/j.scitotenv.2021.152164>.

## References

- Alber, M., 2000. Settleable and non-settleable suspended sediments in the Ogeechee River estuary, Georgia, U.S.A. *Estuar. Coast. Shelf Sci.* 50 (6), 805–816. <https://doi.org/10.1006/ecs.1999.0610>.
- Aminoroayaie Yamini, O., Mousavi, S., Hooman, Kavianpour, M.R., Movahedi, Azin, 2018. Numerical modeling of sediment scouring phenomenon around the offshore wind turbine pile in marine environment. *2018 Environmental Earth Sciences* 77 (23), 1–15. <https://doi.org/10.1007/S12665-018-7967-4> 77 (23).
- Arnaud, G., Mory, M., Abadie, S., Cassen, M., 2009. Use of a resistive rods network to monitor bathymetric evolution in the surf/swash zone. *Journal of Coastal Research* 1781–1785.
- Auld, A.H., Schubel, J.R., 1978. Effects of suspended sediment on fish eggs and larvae: a laboratory assessment. *Estuar. Coast. Mar. Sci.* 6 (2), 153–164. [https://doi.org/10.1016/0302-3524\(78\)90097-X](https://doi.org/10.1016/0302-3524(78)90097-X).
- Barko, John W., Gunnison, Douglas, Carpenter, Stephen R., 1991. Sediment interactions with submersed macrophyte growth and community dynamics. *Aquat. Bot.* 41 (1–3), 41–65. [https://doi.org/10.1016/0304-3770\(91\)90038-7](https://doi.org/10.1016/0304-3770(91)90038-7).
- Chazottes, V., Reijmer, J.J.G., Cordier, E., 2008. Sediment characteristics in reef areas influenced by eutrophication-related alterations of benthic communities and bioerosion processes. *Mar. Geol.* 250 (1–2), 114–127. <https://doi.org/10.1016/j.margeo.2008.01.002>.
- Ćosić-Flajsig, Gorana, Vučković, Ivan, Karleuša, Barbara, 2020. An innovative holistic approach to an E-flow assessment model. *Civil Eng. J.* 6 (11), 2188–2202. <https://doi.org/10.28991/CEJ-2020-03091611>.
- Dyer, Keith R., 1995. Sediment transport processes in estuaries. *Dev. Sedimentol.* 53 (C), 423–449. [https://doi.org/10.1016/S0070-4571\(05\)80034-2](https://doi.org/10.1016/S0070-4571(05)80034-2).
- Gallagher, Edith L., Boyd, William, Elgar, Steve, Guza, R.T., Woodward, Brian, 1996. Performance of a sonar altimeter in the nearshore. *Marine Geology* 133 (3–4), 241–248. [https://doi.org/10.1016/0025-3227\(96\)00018-7](https://doi.org/10.1016/0025-3227(96)00018-7).
- Galloway, Joel M., Evans, Dennis A., Green, W.Reed, 2005. Comparability of suspended-sediment concentration and total suspended-solids data for two sites on the L'Anguille River, Arkansas, 2001 to 2003. *Scientific Investigations Report* <https://doi.org/10.3133/SIR20055193>.
- Håkanson, Lars, 2006. The relationship between salinity, suspended particulate matter and water clarity in aquatic systems. *Ecological Research*. 21. Springer, pp. 75–90. <https://doi.org/10.1007/s11284-005-0098-x>.
- Håkanson, Lars, Floderus, Sören, Wallin, Mats, 1989. Sediment trap assemblages - a methodological description. *Hydrobiologia* 176–177 (1), 481–490. <https://doi.org/10.1007/BF00026583>.
- Hsu, Tai Wen, Lin, Tsung Yi, Fan Tseng, I., 2007. Human impact on coastal erosion in Taiwan. *J. Coast. Res.* 23 (4), 961–973. <https://doi.org/10.2112/04-0353R.1>.
- Hu, Zhan, Lenting, Walther, van der Wal, Daphne, Bouma, Tjeerd J., 2015. Continuous monitoring bed-level dynamics on an intertidal flat: introducing novel, stand-alone high-resolution SED-sensors. *Geomorphology* 245 (September), 223–230. <https://doi.org/10.1016/j.geomorph.2015.05.027>.
- Jestin, H., Bassoullet, P., Hir, P.Le, L'Yavanc, J., Degres, Y., 1998. Development of ALTUS, a high frequency acoustic submersible recording altimeter to accurately monitor bed elevation and quantify deposition or erosion of sediments. *Oceans Conference Record (IEEE)*. 1. IEEE, pp. 189–194. <https://doi.org/10.1109/oceans.1998.725734>.
- Lawler, D.M., 1991. A new technique for the automatic monitoring of erosion and deposition rates. *Water Resour. Res.* 27 (8), 2125–2128. <https://doi.org/10.1029/91WR01191>.
- Matos, T., Faria, C.L., Martins, M.S., Henriques, Renato, Gomes, P.A., Goncalves, L.M., 2019a. Development of a cost-effective optical sensor for continuous monitoring of turbidity and suspended particulate matter in marine environment. *Sensors* 19 (20), 4439. <https://doi.org/10.3390/s19204439>.
- Matos, Tiago, Faria, C.L., Martins, M., Henriques, R., Goncalves, L., 2019b. Optical device for in situ monitoring of suspended particulate matter and organic/inorganic distinguish. *OCEANS 2019 - Marseille, OCEANS Marseille 2019*. 2019-June. Institute of Electrical and Electronics Engineers Inc. <https://doi.org/10.1109/OCEANSE.2019.8867080>.
- Matos, T., Faria, C.L., Martins, M.S., Henriques, Renato, Gomes, P.A., Goncalves, L.M., 2020. Design of a Multipoint Cost-Effective Optical Instrument for Continuous In-Situ Monitoring of Turbidity and Sediment. *Sensors* 20 (11), 3194. <https://doi.org/10.3390/s20113194>.

- Rabeni, Charles F., Smale, Martin A., 1995. Effects of siltation on stream fishes and the potential mitigating role of the buffering riparian zone. *Hydrobiologia* 303 (1–3), 211–219. <https://doi.org/10.1007/BF00034058>.
- Rachold, Volker, Grigoriev, Mikhail N., Are, Felix E., Solomon, Steve, Reimnitz, Erk, Kassens, Heidemarie, Antonow, Martin, 2000. Coastal erosion vs riverline sediment discharge in the Arctic shelf seas. *Int. J. Earth Sci.* 89 (3), 450–460. <https://doi.org/10.1007/s005310000113>.
- Ridd, Peter V., 1992. A sediment level sensor for erosion and siltation detection. *Estuar. Coast. Shelf Sci.* 35 (4), 353–362. [https://doi.org/10.1016/S0272-7714\(05\)80032-0](https://doi.org/10.1016/S0272-7714(05)80032-0).
- Ridd, P., Day, G., Thomas, S., Harradence, J., Fox, D., Bunt, J., Renagi, O., Jago, C., 2001. Measurement of sediment deposition rates using an optical backscatter sensor. *Estuar. Coast. Shelf Sci.* 52 (2), 155–163. <https://doi.org/10.1006/ecss.2000.0635>.
- Rooij, F.De, Dalziel, S.B., Linden, P.F., 1999. Electrical measurement of sediment layer thickness under suspension flows. *Experiments in Fluids* 26 (5), 470–474. <https://doi.org/10.1007/s003480050311>.
- Storlazzi, C.D., Field, M.E., Bothner, M.H., 2011. The use (and Misuse) of sediment traps in coral reef environments: theory, observations, and suggested protocols. *Coral Reefs* 30 (1), 23–38. <https://doi.org/10.1007/s00338-010-0705-3>.
- Thomas, Séverine, Ridd, Peter, 2005. “Field assessment of innovative sensor for monitoring of sediment accumulation at inshore coral Reefs”. In: *Mar. Pollut. Bull.* 51 (470–80), Pergamon. <https://doi.org/10.1016/j.marpolbul.2004.10.026>.
- Tuckerman, Steve, Zawiski, Bill, 2007. Case studies of dam removal and TMDLs: process and results. *J. Great Lakes Res.* 33 (January), 103–116. [https://doi.org/10.3394/0380-1330\(2007\)33\[103:CSODRA\]2.0.CO;2](https://doi.org/10.3394/0380-1330(2007)33[103:CSODRA]2.0.CO;2).
- Van Rijn, L.C., 2011. Coastal erosion and control. *Ocean Coast. Manag.* 54 (12), 867–887. <https://doi.org/10.1016/j.ocecoaman.2011.05.004>.
- van der Wal, Daphne, Forster, Rodney M., Rossi, Francesca, Hummel, Herman, Ysebaert, Tom, Roose, Frederik, Herman, Peter M.J., 2011. Ecological evaluation of an experimental beneficial use scheme for dredged sediment disposal in shallow tidal waters. *Mar. Pollut. Bull.* 62 (1), 99–108. <https://doi.org/10.1016/J.MARPOLBUL.2010.09.005>.
- Wenger, Amelia S., McCormick, Mark I., Endo, Geoffrey G.K., McLeod, Ian M., Kroon, Frederieke J., Jones, Geoffrey P., 2014. Suspended sediment prolongs larval development in a coral reef fish. *J. Exp. Biol.* 217 (7), 1122–1128. <https://doi.org/10.1242/jeb.094409>.
- Whinney, James, Jones, Ross, Duckworth, Alan, Ridd, Peter, 2017. Continuous in situ monitoring of sediment deposition in shallow benthic environments. *Coral Reefs* 36 (2), 521–533. <https://doi.org/10.1007/s00338-016-1536-7>.
- Wilson, W.Herbert, 1990. Competition and predation in marine soft-sediment communities. *Annu. Rev. Ecol. Syst.* 21 (1), 221–241. <https://doi.org/10.1146/annurev.es.21.110190.001253>.
- Yang, Z., Wang, H., Saito, Y., Milliman, J.D., Xu, K., Qiao, S., Shi, G., 2006. Dam impacts on the changjiang (Yangtze) river sediment discharge to the sea: the past 55 years and after the three gorges dam. *Water Resour. Res.* 42 (4), 4407. <https://doi.org/10.1029/2005WR003970>.